

“Thermal Charging” Phenomenon in Electrical Double Layer Capacitors

Jianjian Wang,[†] Shien-Ping Feng,^{†,‡} Yuan Yang,[†] Nga Yu Hau,[‡] Mary Munro,[†] Emerald Ferreira-Yang,[†] and Gang Chen^{*,†}

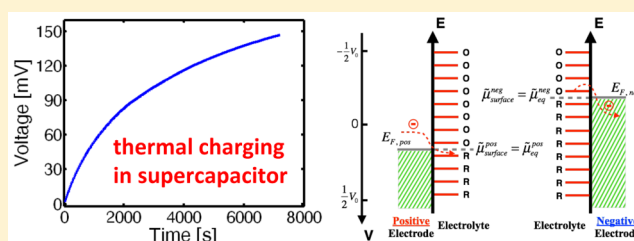
[†]Department of Mechanical Engineering, Massachusetts Institute of Technology, 77 Massachusetts Avenue, Cambridge, Massachusetts 02139, United States

[‡]Department of Mechanical Engineering, The University of Hong Kong, Pokfulam, Hong Kong

S Supporting Information

ABSTRACT: Electrical double layer capacitors (EDLCs) are usually charged by applying a potential difference across the positive and negative electrodes. In this paper, we demonstrated that EDLCs can be charged by heating. An open circuit voltage of 80–300 mV has been observed by heating the supercapacitor to 65 °C. The charge generated at high temperature can be stored in the device after its returning to the room temperature, thus allowing the lighting up of LEDs by connecting the “thermally charged” supercapacitors in a series. The underlying mechanism is related to a thermo-electrochemical process that enhances the kinetics of Faradaic process at the electrode surface (e.g., surface redox reaction of functional group, or chemical adsorption/desorption of electrolyte ions) at higher temperature. Effects of “thermal charging” times, activation voltage, rate, and times on “thermally charged” voltage are studied and possible mechanisms are discussed.

KEYWORDS: Supercapacitor, “thermal charging”, electrical double layer, surface functional group, surface redox reaction, chemical adsorption/desorption



An electrical double layer capacitor (EDLC), also known as a supercapacitor, stores energy in the electrical double layer at the electrolyte/electrode interface through reversible charge adsorption/desorption.^{1,2} EDLCs are attractive for energy storage as they have high specific capacitance (>100F/g), long cycle life (>500 000), and simple operating principle.³ Currently, supercapacitors have applications in consumer electronics, memory back-up systems, and as a means of supplementing high and frequent peaks in power demand.^{4,5} It also has potential application in electric vehicles for complementing batteries or fuel cells to improve power density.⁶ Moreover, flexible, printable, and wearable supercapacitors can be potentially integrated into smart clothing, sensors, wearable electronics.⁷

Capacitive behavior can be classified into two categories, electrochemical double-layer capacitance (EDLC) and pseudocapacitance. EDLC is a nonfaradaic process based on the electrostatic separation of charges at the electrode/electrolyte interface, whereas pseudocapacitance is a faradaic process (surface redox reaction of functional group, or chemical adsorption/desorption of electrolyte ions) involving electron transfer across the double layer at the electrode/electrolyte interface.^{1,4,8,9} These two charge storage mechanisms can function simultaneously in supercapacitors when an electrical potential differential is applied between two electrodes. The most common commercially available supercapacitor is comprised of two carbon electrodes (one positive and one

negative) separated by a porous separator. The electrodes and separator are impregnated with organic (e.g., acetonitrile-based or carbonate-based) electrolytes. The charge storage mechanisms of the supercapacitor are a function of the electrical potential (potential-dependent), which have been extensively investigated.^{10–14} Temperature also plays an important role in electrochemical reactions. For example, electrolyte ion adsorption/desorption can still occur without the application of an electrical potential difference, depending on electrochemical kinetics in such a way that the reaction (e.g., adsorption/desorption) rate enhanced with increased temperature. While adsorption processes are exothermic in most cases,¹⁵ there are also literatures reporting endothermic adsorption processes on activated carbon surface,^{16–18} which may be attributed to¹⁸ the enhanced penetration of adsorbates into micropores of activated carbon due to the reduced electrolyte viscosity¹⁹ or the creation of a new active site on the activated carbon surface at higher temperatures. One past work on temperature-dependent effect on supercapacitor voltage is that of Qiao et al.^{20,21} who observed a transient voltage when the two identical porous electrodes of an EDLC were placed at different temperatures (one electrode was kept at low

Received: May 5, 2015

Revised: July 25, 2015

Published: August 3, 2015

temperature, and the other one was kept at high temperature), and they interpreted the origin of the voltage as a result of the temperature-dependent ion density near the electrode surface. However, it is not clear how the surface Faradaic process, such as the redox reaction of functional groups, affects the results.

In this paper, we report a “thermal charging” phenomenon in supercapacitors that an electrically charged and discharged EDLC can develop a voltage in open circuit condition, and this voltage builds up at a much faster speed when it was heated, which is likely a result of kinetically governed surface faradaic process, such as redox reaction of surface functional group or chemical adsorption/desorption. The generated capacitance can be stored in the system after returning to room temperature. Results on such “thermal charging” behavior are presented and possible mechanisms are also discussed.

All of our experiments were carried out using commercial EDLCs. A Gamry PCI4/300 potentiostat/galvanostat was used in the electrochemical measurement with a two-electrode configuration. A new EDLC was first shorted for 15 min to ensure that its initial open circuit voltage (OCV) is 0 mV. Then the capacitor was electrically charged and discharged (Figure 1a) with a constant current (e.g., 10 mA), which was a necessary activation step in order to observe the “thermal charging” phenomenon. The next step was to short the capacitor at room temperature for half an hour to equilibrate the system. Then the capacitor was soaked in a hot water bath (e.g., 65 °C) and the OCV of the capacitor slowly increased (e.g., reaching 80–300 mV within 2 h). Figure 1b shows an example of this “thermal charging” phenomenon for a capacitor (Maxwell 2.7 V 5F) with and without one cycle of electrical charge/discharge, which we call the activation cycle. For the sample with one activation cycle, OCV rose to ~50 mV after 1000 s and increased slowly to ~140 mV after 7000 s. The voltage remains the same after cooling the capacitor from 65 °C to room temperature. Figure S1 shows that the self-discharge in a “thermally charged” EDLC is negligible. Moreover, the capacitance of the capacitor after “thermal charging” is similar to that in normal electrical charge/discharge (Figure S2). If we connect these “thermally charged” EDLCs in series with each other, they are capable of lighting up a few LEDs. In contrast, OCV of a capacitor without the electrical charge/discharge activation cycle only fluctuates in the order of microvolts (Figure 1b).

Such “thermal charging” phenomenon has been observed in several different types of commercial EDLCs, as shown in Figure S3. All four types of capacitors exhibit the “thermal charging” phenomenon, although they show different “thermally charged” voltage, which may be attributed to the detailed compositions of functional groups on electrode surface and electrolyte composition, as we will explain in more details below. Therefore, we believe that this “thermal charging” of EDLC is a universal phenomenon. The major components of the commercial EDLCs used for our experiments are activated carbon for electrode material and acetonitrile or propylene carbonate for electrolyte material,²² although we do not have detailed compositional information on these commercial EDLCs. Table S1 also lists some widely used electrode and electrolyte materials in EDLCs.

To understand the underlying mechanism, we first studied effect of temperature on the “thermal charging” behavior. The OCV–time curves up to 60 h were recorded for capacitors rested at room temperature (~24 °C) and heated to 65 °C after one electrical charge/discharge cycle (Figure 1c). In both

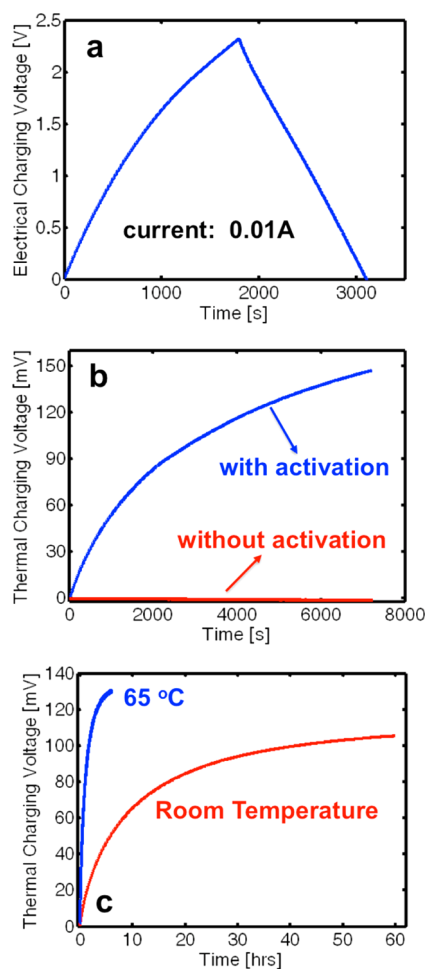


Figure 1. Thermal charging phenomenon in an EDLC. (a) Activation step before “thermal charging” through electrical charging and discharging of an EDLC (Maxwell 2.7 V 5F) at a constant current (0.01A); (b) Thermal charging of a capacitor with and without the activation step. The blue curve is the evolution of OCV upon time after soaking an activated capacitor in hot water (65 °C). The voltage gradually increases to ~150 mV within 2 h. The red curve is the OCV–time plot of a capacitor in hot water without electrical activation step in (a). The OCV only fluctuates on the order of microvolts. (c) Comparison of “thermal charging” processes of the same type EDLC at 65 °C and room temperature. Both capacitors can be “thermally charged” to similar voltage (~131 mV at 65 °C vs ~105 mV at room temperature) but the process at room temperature requires significantly longer time.

cases, recovery of voltage was observed and the recovery speed gradually slowed down upon time. However, the time scale was very different. At 65 °C, the time to reach 50 mV was only about 1500 s while it was about 2×10^4 s at room temperature. Although the voltage did not fully saturate at the end of our measurement, the final values were clearly close (~131 mV for 65 °C and ~105 mV for room temperature). Such distinct time scales and similar observed “thermally charged” voltages suggest that the phenomenon is a kinetic process rather than a thermodynamic process.

We interpret such a phenomenon to be a result of improved kinetics of the sluggish surface Faradaic processes at high temperatures, so that the capacitor voltage can approach the thermodynamic equilibrium voltage (which is the final achievable voltage as long as the time for “thermal charging” is sufficiently long) faster (Figure S4 clearly shows the increased

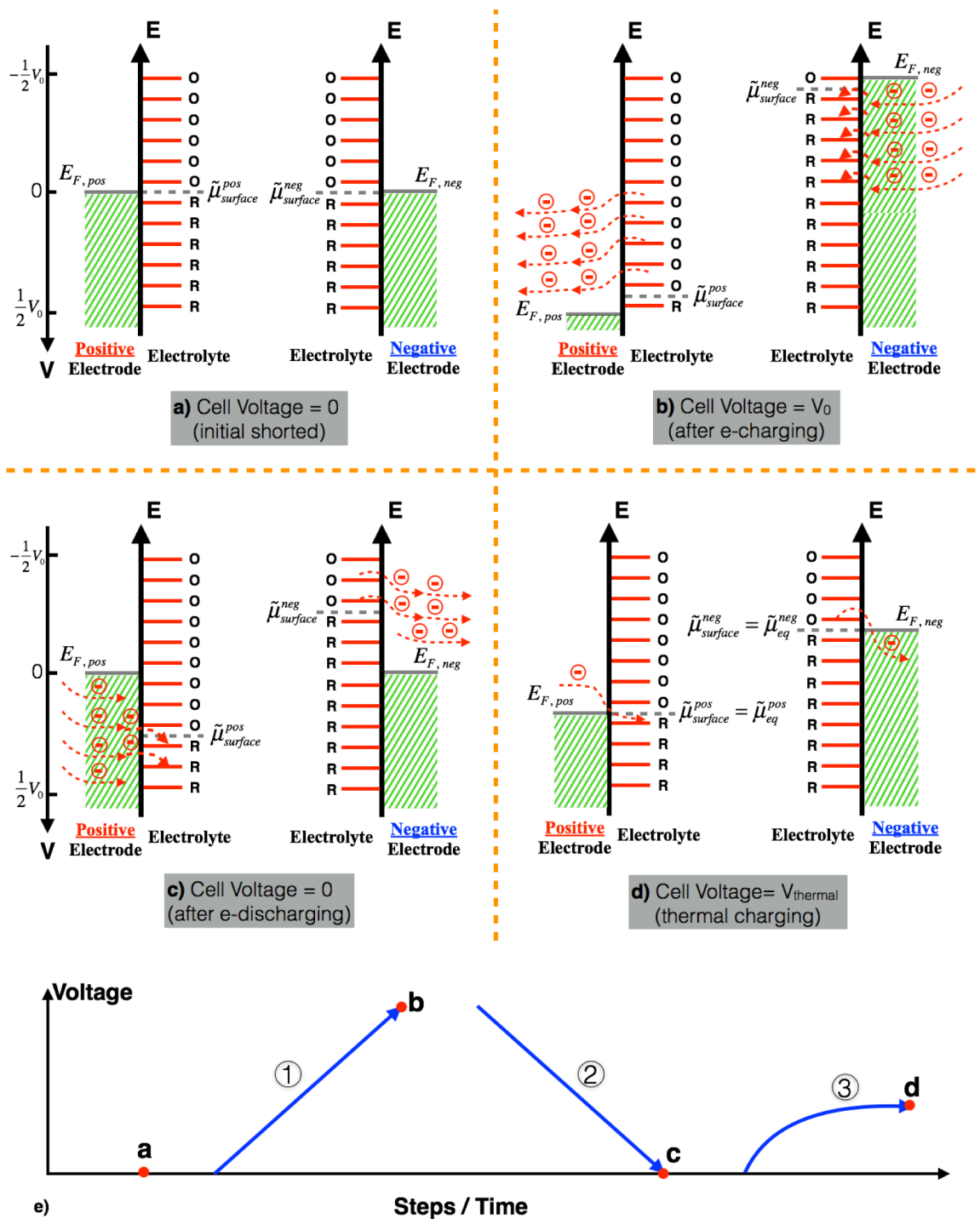


Figure 2. Schematic of the mechanism of “thermal charging”. Fermi-level in electrode is represented as gray line and denoted as E_F . The difference between the $E_{F, \text{pos}}$ and $E_{F, \text{neg}}$ is read as the EDLC voltage. The slash lines indicate that the part below Fermi-level is occupied by electrons as the positive y-axis is energy and the negative y-axis is voltage. Functional groups are represented by red lines. R and O indicate reduced and oxidized states, respectively. The average energy level between O state with lowest energy and R state with highest energy is defined as electrochemical potential of surface redox reaction ($\tilde{\mu}_{\text{surface}}$). (a) The initial cell voltage of an EDLC after shorting is 0 mV, which corresponds to state a in (e). At the beginning, the functional groups with energy lower than $E_{F, \text{pos}}$ are fully reduced in the positive electrode, while the functional groups with energy higher than $E_{F, \text{neg}}$ are fully oxidized in the negative electrode. (b) The EDLC is electrically charged to a high voltage V_0 , which corresponds to the process 1 in (e). During the charging process, electrons are removed from the positive electrode and flow into the negative electrode. Most of the functional groups with reaction potential lower than $V_0/2$ are oxidized in the positive electrode, while most of the functional groups with reaction potential higher than $-V_0/2$ are reduced in the negative electrode. Therefore, in the electrical charging process some of electrical energy is converted into chemical energy. (c) The EDLC is then electrically discharged and shorted at 0 mV again, which corresponds to process 2 in (e). During this process, electrons flow into the positive electrode and are removed from the negative electrode. Part of the oxidized/reduced functional groups on the positive/negative electrode are reduced/oxidized due to the sluggish reaction kinetics of functional group, but many are left in the oxidized/reduced state. (d) The process of “thermal charging” EDLC in hot water (65 °C), which corresponds to the process 3 in (e). At high temperature, reaction kinetics of functional groups is improved. In the positive electrode, electrons with energy higher (or potential lower) than that

Figure 2. continued

of oxidized functional groups (O state) can be transferred to the oxidized functional groups, hence reducing them. While in the negative electrode, electrons stored in the reduced functional groups (R state) with energy higher (potential lower) than $E_{F,neg}$ will be transferred to the bulk of electrode, hence oxidizing them. As a result, Fermi level in the positive electrode ($E_{F,pos}$) moves toward more positive potential and finally equilibrates with that of surface functional groups $\tilde{\mu}_{eq}^{pos}$, and the Fermi level in the negative electrode ($E_{F,neg}$) moves toward more negative potential and finally equilibrates with that of surface functional groups $\tilde{\mu}_{eq}^{neg}$, which is reflected as “thermal charging” phenomenon and the EDLC develops a “thermally charged” voltage ($V_{thermal} = (E_{F,pos} - E_{F,neg})/e = (\tilde{\mu}_{eq}^{pos} - \tilde{\mu}_{eq}^{neg})/e$).

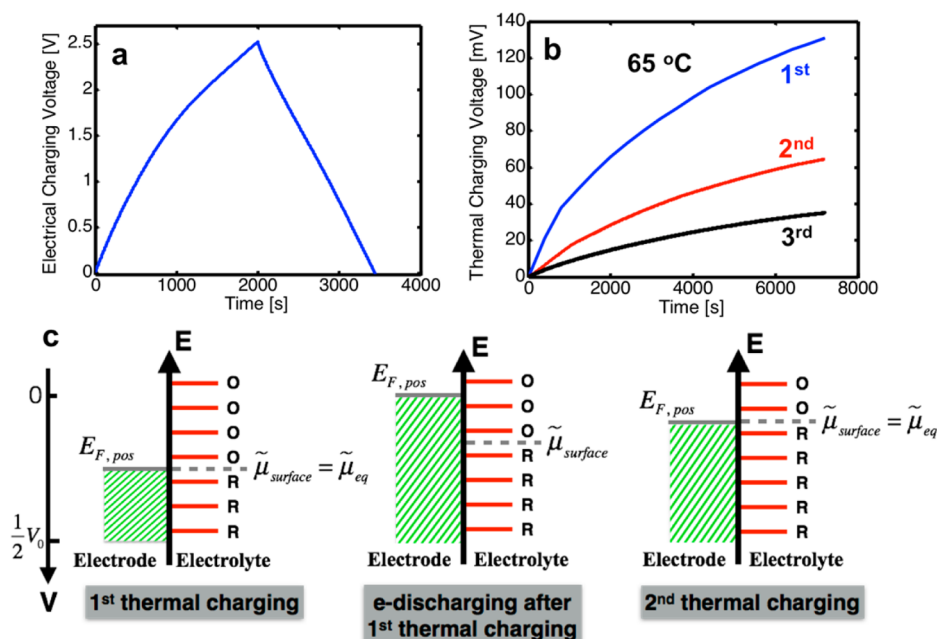


Figure 3. Experimental results and schematics of multiple “thermal charging” after single electrical charging/discharging activation cycle (only the positive electrode is illustrated). (a) Activation step before “thermal charging”; (b) multiple “thermal charging”. The blue curve is the first “thermal charging” of the EDLC in hot water after activation and shorting steps, which shows the largest “thermally charged” voltage. The red and black curves are the second and third “thermal charging” of the EDLC, respectively. The EDLC is discharged to 0 mV after each “thermal charging” at room temperature. (c) Corresponding mechanisms of reduced “thermally charged” voltage in multiple “thermal charging”. As oxidized functional groups with high reaction potential is reduced first, the reaction potential of functional groups in the oxidized state become lower in subsequent “thermal charging”. As a result, in second and third “thermal charging” the voltage of electrons in electrodes can only be recovered to a lower value.

“thermal charging” speed as the temperature gradually increases). Before explaining the mechanism, we would like to discuss briefly on the nature of surface Faradaic processes. The surface Faradaic processes could be either redox reaction of surface functional groups ($O + ne^- \leftrightarrow R$), where O is the oxidized state and R is the reduced state, or chemical adsorption/desorption ($M^{z+} + ze^- + S \leftrightarrow MS$), where M^{z+} is the absorbed ion and S indicates surface site. The existence of functional groups and chemical adsorption processes mainly comes from the pretreatments (such as heat and acid treatments) of carbon materials used in the EDLCs.^{23,24} Common functional groups at the carbon materials surface include ortho-quinonoid, ketone, phenolic, carbinol, lactone, o-hydroquinoid, and so forth,^{1,25} and the exact chemistry is determined by detailed properties of electrode surface and electrolyte composition. Nevertheless, electrons move across the electrode/electrolyte interface in both cases and the chemical species involved switch between the state without electron (O or M^{z+}/S) and with electron (R or MS). Therefore, in the following discussions O and R are used to represent the two states in the surface Faradaic process for simplicity. The same mechanism illustrated below can be applied to chemical adsorption/desorption too.

The detailed mechanism is illustrated in Figure 2 to show the electrode potential and electronic energy diagram of both positive and negative electrodes during each experimental procedure. The difference between the energy levels of electron in the positive ($E_{F,pos}$) and negative ($E_{F,neg}$) electrodes determines the instant voltage of EDLC. Because the analysis of positive and negative electrodes is similar, for simplicity we just use the positive electrode as an example (the left figures of Figure 2a–d) to illustrate the “thermal charging” mechanism here and in the following experiments. During electrical charging (step 1 from Figure 2a,b), electrons are removed from the positive electrode, so the Fermi level ($E_{F,pos}$) moves down and the electrode potential goes up, as indicated by the voltage axis. Meanwhile, surface functional groups at different energy levels are oxidized to the O state. The average energy level between O state with lowest energy and R state with highest energy is defined as electrochemical potential of surface redox reaction ($\tilde{\mu}_{surface}^{pos}$), as indicated by the dash line in Figure 2a–d. $E_{F,pos}$ equals to $\tilde{\mu}_{surface}^{pos}$ before charging. However, because the kinetics of surface reactions is slower than the fast free electron flow in the electrode, $\tilde{\mu}_{surface}^{pos}$ is slightly higher than $E_{F,pos}$. In the discharge and the following shorting step (step 2 from Figure 2b,c), electrons flow into the positive electrode. As the surface Faradaic reactions have a slow kinetics and poor

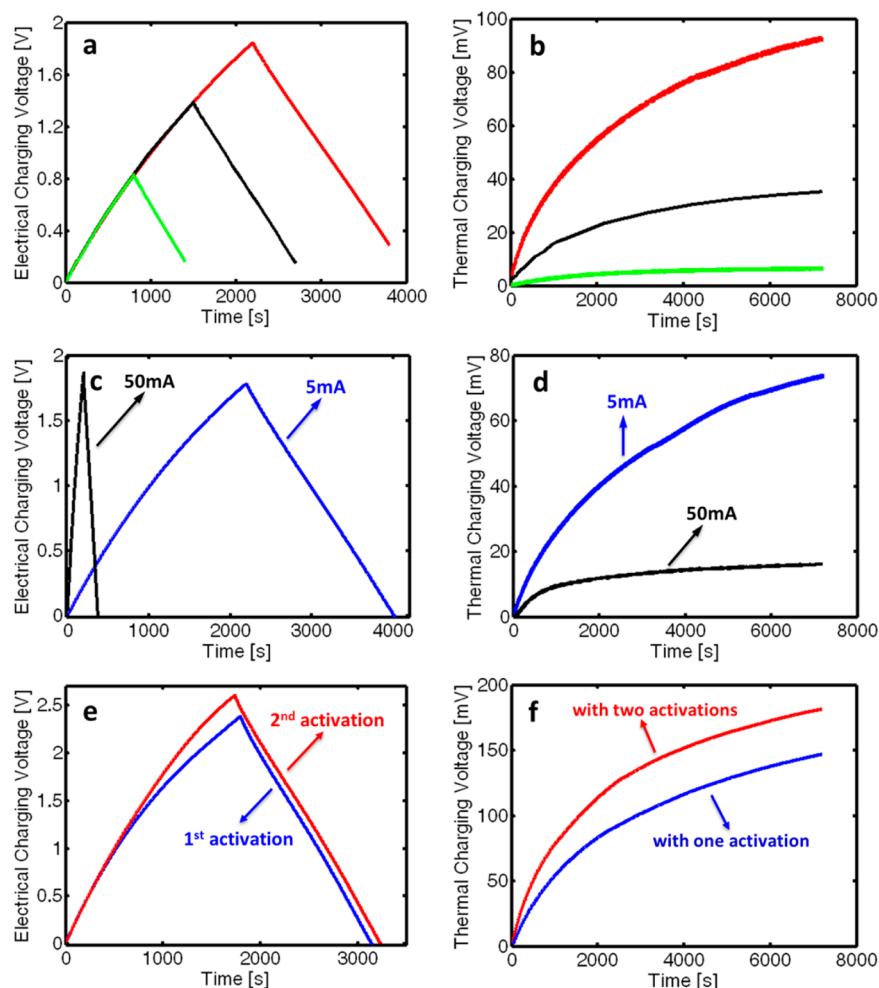


Figure 4. Effects of electrical charging voltage cutoff, electrical current rates, and multiple electrical charging (or multiple activations) on the “thermally charged” voltage. (a) Voltage profiles of the activation step with different electrical charging voltage cutoff. The red, black, and green curves are electrically charged to 1.85, 1.39, and 0.83 V, respectively. (b) The corresponding three “thermal charging” curves. Higher electrical charging voltage cutoff in the activation step results in higher “thermally charged” voltage. (c) Voltage profiles of activation step with different electrical charging currents. The black and blue ones correspond to 50 and 5 mA, respectively. (d) The corresponding “thermally charged” voltage curves. Slower electrical charging current during the activation step results in higher “thermally charged” voltage. (e) Blue line represents a capacitor with only one activation, and red line represents the same type capacitor with two activations (charge/discharge cycle). (f) The corresponding “thermal charging” curves of these two EDLCs treated with different times of activation. Two activations result in higher “thermally charged” voltage.

reversibility, only part of functional groups are reduced to the R state. The functional groups with the highest electrode potential (lowest electrochemical potential) should be reduced first as the overpotential is large. As a result, $\bar{\mu}_{\text{surface}}^{\text{pos}}$ is much lower than $E_{\text{F, pos}}$ (Figure 2c). They will try to align with each other through the sluggish surface Faradaic process; thus $E_{\text{F, pos}}$ slowly moves down, which corresponds to that the electrode potential of positive electrode becomes more positive (step 3 from Figure 2c,d). Heating capacitor at an elevated temperature improves the kinetics of step 3 so that the voltage recovery is at a much faster speed. Here it should be noticed that the kinetics includes not only the charge transfer process at electrolyte/electrode interface but also other processes involved in the reaction, such as diffusion of reactants in electrolytes (in the chemical adsorption/desorption case, another factor that contributes to the faster voltage recovery speed at higher temperature is the faster ion diffusion rate because the electrolyte viscosity is reduced at higher temperature¹⁹). However, because the final equilibrium electrochemical potential is determined by the amount of surface functional

groups that remained in the O state after initial discharge/shorting step (Figure 2c), the final equilibrium electrochemical potential ($\bar{\mu}_{\text{eq}}^{\text{pos}}$ in Figure 2d), although may take quite long time to reach, should be the same for “thermal charging” at 65 °C and resting at room temperature, as observed in Figure 1c. Similarly, the Fermi level of electrons in the negative electrode, $E_{\text{F, neg}}$ moves toward more negative voltages in “thermal charging”, and thus the full cell voltage of capacitor increases in this “thermal charging” process.

This mechanism is also consistent with many other experimental results, such as the attenuation of the “thermally charged” voltage in successive “thermal charging” processes for one electrical charging/discharging activation cycle, the dependence of “thermally charged” voltage on electrical charging voltage cutoff, electrical charging current rate, and electrical charging times. For example, Figure 3 shows three consecutive “thermal charging” curves at 65 °C after one electrical charging/discharging activation cycle. After each “thermal charging”, the capacitor was discharged to 0 mV at room temperature and followed by shorting for half an hour.

Then it was soaked in hot water at 65 °C again and the OCV was recorded. Clearly the “thermally charged” voltage becomes smaller after each “thermal charging” cycle. This phenomenon can be explained as follows (we will just illustrate the positive electrode for simplicity, and here and later on all the $\tilde{\mu}_{\text{surface}}$ and $\tilde{\mu}_{\text{eq}}$ are for positive electrode). After first “thermal charging”, $E_{\text{F, pos}}$ and $\tilde{\mu}_{\text{eq}}$ are aligned with each other (Figure 3c). In the following discharge, both $E_{\text{F, pos}}$ and $\tilde{\mu}_{\text{surface}}$ move up, but $\tilde{\mu}_{\text{surface}}$ is lower than $E_{\text{F, pos}}$ due to the sluggish nature of surface Faradaic processes. Then $E_{\text{F, pos}}$ and $\tilde{\mu}_{\text{surface}}$ will try to align with each other in the second “thermal charging” and $\tilde{\mu}_{\text{eq}}$ moves up. As a higher electrochemical potential corresponds to a lower voltage, the “thermally charged” voltage gradually decreases in multiple “thermal charging”.

The “thermally charged” voltage also depends on details of the electrical charging process (e.g., electrical charging voltage cutoff, electrical charging speed, and electrical charging times). For example, one of the observations is that the “thermally charged” voltage is higher if the capacitor was electrically charged to a higher voltage (Figure 4a,b). This is because more surface functional groups at higher electrode potential (lower electrochemical potential) can be oxidized. As a result, after electrical discharging, $\tilde{\mu}_{\text{surface}}$ is lower. Therefore, after $E_{\text{F, pos}}$ and $\tilde{\mu}_{\text{surface}}$ align with each other to reach the equilibrium, $\tilde{\mu}_{\text{eq}}$ is lower for the capacitor with higher charging voltage cutoff, which corresponds to higher “thermally charged” voltage (see Figure S5 in Supporting Information for more details).

Another observation is that faster electrical charging/discharging leads to smaller “thermally charged” voltage (Figure 4c,d). This can be explained by the fact that less functional groups are oxidized during fast charging. The oxidation of surface functional groups has several steps including diffusion of reactants involved in electrolyte (e.g., dissolved O₂, H₂O, or ions), charge transfer across electrolyte/electrode interface and electron transfer in the carbon matrix. At a fast electrical charging/discharging rate, diffusion of reactants involved could be the limiting step for reaction rate and thus less functional groups are oxidized in fast electrical charging. Kinetics of charge transfer step could also reduce the amount of functional groups oxidized, depending on its characteristic time scale. As a result, when the electrical charging process is slow (Figure S6c), more functional groups can be oxidized, especially at high electrode potential (low electrochemical potential). After electrical discharging, more functional groups in the oxidized state will be left at the electrode surface and $\tilde{\mu}_{\text{surface}}$ is lower. In contrast, when the electrical charging process is fast (Figure S6d), more functional groups in the reduced state do not have enough time to be oxidized, especially for those with high electrode potential (low electrochemical potential). After the electrical discharging step, less functional groups in the oxidized state are left at the electrode surface and $\tilde{\mu}_{\text{surface}}$ is higher. Therefore, $\tilde{\mu}_{\text{eq}}$ is lower when the electrical charging rate is low, which corresponds to higher “thermally charged” voltage at small charge/discharge current.

The times of electrical charging/discharging (activation) also affect the “thermally charged” voltage. Multiple activation times result in higher “thermally charged” voltage (Figure 4e,f). When the EDLC was activated twice, more functional groups are left in oxidized state (middle scheme in Figure S7d), as some functional groups have already been oxidized after the first activation (charge/discharge) process (middle scheme in Figure S7c). Therefore, after two activations more functional groups were at oxidized states compared to only one activation.

Consequently $\tilde{\mu}_{\text{eq}}$ is lower and the final “thermally charged” voltage of EDLC with twice activations would be higher than that with one single activation (see Figure S7 in Supporting Information for more details).

In summary, we report a “thermal charging” phenomenon in EDLCs that the voltage of an EDL capacitor can be recovered much faster by heating. This “thermal charging” effect is related to the surface redox reaction of functional group or chemical adsorption/desorption of electrolyte ions resulting from the electrochemical reactions between the specific functional groups on the surface of activated carbon or/and electrolyte ions via a prior electrical charge/discharge activation step.

■ ASSOCIATED CONTENT

Supporting Information

The Supporting Information is available free of charge on the ACS Publications website at DOI: 10.1021/acs.nanolett.5b01761.

Demonstration of negligible self-discharge demonstration in “thermally charged” EDLC, capacitance measurement of “thermally charged” EDLC, “thermal charging” demonstration in different types of commercial EDLCs, temperature-dependent “thermal charging” speed, detailed mechanism explanation for factors that affecting the “thermally charged” voltage, and an additional table. (PDF)

■ AUTHOR INFORMATION

Corresponding Author

*E-mail: gchen2@mit.edu.

Notes

The authors declare no competing financial interest.

■ ACKNOWLEDGMENTS

This project started with a few high school students’ summer projects, including Scott Chen, Bushi Ren, and Silong Yang. Funding for this work is primarily provided by “Solid State Solar-Thermal Energy Conversion Center (S³TEC)”, an Energy Frontier Research Center funded by the U.S. Department of Energy, Office of Science, Office of Basic Energy Sciences under Award Number DE-SC0001299/DE-FG02-09ER46577 (G.C.). Work at HKU was also partially supported by the General Research Fund from Research Grants Council of Hong Kong Special Administrative Region, China, under Award Number 17202314 (S.-P.F.). The authors also thank Dr. Yanfei Xu for her comments on the manuscript and Vazrik Chiloyan for proofreading the manuscript.

■ REFERENCES

- (1) Conway, B. E. *Electrochemical Supercapacitors*; Springer: New York, 1999.
- (2) Qu, D.; Shi, H. *J. Power Sources* **1998**, *74*, 99–107.
- (3) Burke, A. *Electrochim. Acta* **2007**, *53*, 1083–1091.
- (4) Zhang, L. L.; Zhao, X. S. *Chem. Soc. Rev.* **2009**, *38*, 2520–2531.
- (5) Kötz, R.; Carlen, M. *Electrochim. Acta* **2000**, *45*, 2483–2498.
- (6) Faggioli, E.; Rena, R.; Danel, V.; Andrieu, X.; Mallant, R.; Kahlen, H. *J. Power Sources* **1999**, *84*, 261–269.
- (7) Kaempgen, M.; Chan, C. K.; Ma, J.; Cui, Y.; Gruner, G. *Nano Lett.* **2009**, *9*, 1872–1876.
- (8) Simon, P.; Gogotsi, Y. *Nat. Mater.* **2008**, *7*, 845–854.
- (9) Qu, D. *J. Power Sources* **2002**, *109*, 403–411.
- (10) Toupin, M.; Brousse, T.; Bélanger, D. *Chem. Mater.* **2004**, *16*, 3184–3190.

- (11) Conway, B. E. *J. Electrochem. Soc.* **1991**, *138*, 1539–1548.
- (12) Nam, K.-W.; Kim, K.-B. *J. Electrochem. Soc.* **2002**, *149*, A346–A354.
- (13) Stoller, M. D.; Park, S.; Zhu, Y.; An, J.; Ruoff, R. S. *Nano Lett.* **2008**, *8*, 3498–3502.
- (14) Largeot, C.; Portet, C.; Chmiola, J.; Taberna, P.-L.; Gogotsi, Y.; Simon, P. *J. Am. Chem. Soc.* **2008**, *130*, 2730–2731.
- (15) Ruthven, D. M. *Principles of adsorption and adsorption processes*; Wiley-Interscience: New York, 1984.
- (16) Namasivayam, C.; Kavitha, D. *Dyes Pigm.* **2002**, *54*, 47–58.
- (17) Moreira, R.; Kuhnen, N.; Peruch, M. *Lat. Am. Appl. Res.* **1998**, *28*, 37–41.
- (18) Al-Degs, Y. S.; El-Barghouthi, M. I.; El-Sheikh, A. H.; Walker, G. *M. Dyes Pigm.* **2008**, *77*, 16–23.
- (19) Ma, L.; Wang, J. J.; Marconnet, A. M.; Barbati, A. C.; McKinley, G. H.; Liu, W.; Chen, G. *Nano Lett.* **2015**, *15*, 127–133.
- (20) Qiao, Y.; Punyamurtual, V. K.; Han, A.; Lim, H. J. *Power Sources* **2008**, *183*, 403–405.
- (21) Lim, H.; Lu, W.; Chen, X.; Qiao, Y. *Nanotechnology* **2013**, *24*, 465401–465405.
- (22) Simon, P.; Burke, A. *Electrochem. Soc. Interface* **2008**, *17*, 38–43.
- (23) Pandolfo, A. G.; Hollenkamp, A. F. *J. Power Sources* **2006**, *157*, 11–27.
- (24) Chu, X.; Kinoshita, K. *Mater. Sci. Eng., B* **1997**, *49*, 53–60.
- (25) Sereydyh, M.; Hulicova-Jurcakova, D.; Lu, G. Q.; Bandosz, T. J. *Carbon* **2008**, *46*, 1475–1488.